Medical Physics
The International Journal of Medical Physics Research and Practice

Computation of energy imparted in diagnostic radiology

Nikolaos A. Gkanatsios and Walter Huda

Citation: Medical Physics **24**, 571 (1997); doi: 10.1118/1.597939
View online: http://dx.doi.org/10.1118/1.597939
View Table of Contents: http://scitation.aip.org/content/aapm/journal/medphys/24/4?ver=pdfcov
Published by the American Association of Physicists in Medicine

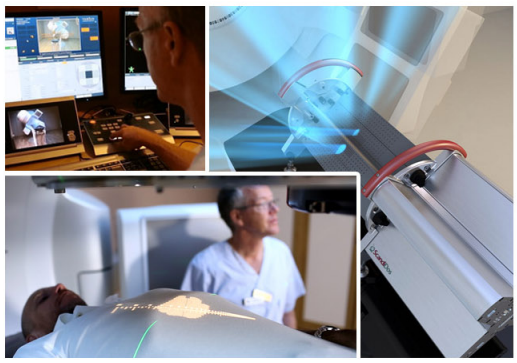

Computation of energy imparted in diagnostic radiology

Nikolaos A. Gkanatsios and Walter Huda[a)]
Department of Radiology, University of Florida College of Medicine, P.O. Box 100374, Gainesville, Florida 32610-0374

(Received 19 June 1996; accepted for publication 23 January 1997)

Energy imparted is a measure of the total ionizing energy deposited in the patient during a radiologic examination and may be used to quantify the patient dose in diagnostic radiology. Values of the energy imparted per unit exposure-area product, $\omega(z)$, absorbed by a semi-infinite water phantom with a thickness z, were computed for x-ray spectra with peak x-ray tube voltages ranging from 50–140 kV and with added filtration, ranging from 1–6 mm aluminum. For a given phantom thickness and peak x-ray tube voltage, the energy imparted was found to be directly proportional to the x-ray beam half-value layer (HVL) expressed in millimeters of aluminum. Values of $\omega(z)$ were generated for constant waveform x-ray tube voltages and an anode angle of 12°, and were fitted to the expression $\omega(z) = \alpha \times \mathrm{HVL} + \beta$. Fitted α and β parameters are provided that permit the energy imparted to be determined for any combination of tube voltage, half-value layer, and phantom thickness from the product of the entrance skin exposure (free-in-air) and the corresponding x-ray beam area. The results obtained using our method for calculating energy imparted were compared with values of energy imparted determined using Monte Carlo techniques and anthropomorphic phantoms for a range of diagnostic examinations. At 60, 80, and 120 kV, absolute values of energy imparted obtained using our method differed by 8%, 10%, and 12%, respectively, from the corresponding results of Monte Carlo computations obtained for an anthropomorphic phantom. The method described in this paper permits a simple determination of energy imparted for any type of diagnostic x-ray examination which may be used to compare the radiologic risks from differing types of x-ray examinations, optimize imaging techniques with respect to the patient dose, or estimate the patient effective dose equivalent. [S0094-2405(97)01304-7]

Key words: integral dose, energy imparted, waveform ripple, anode angle, patient dosimetry

I. INTRODUCTION

Although the entrance skin exposure has been a popular method of expressing patient radiation doses, this parameter does not take into account the x-ray beam quality [i.e., half-value layer (HVL)] or the size of the x-ray beam. As a result, the patient exposure is generally a poor indicator of the risk associated with a given radiologic examination. In recent times, the effective dose equivalent, H_E,[1] and the effective dose, E,[2] have been used to quantify the dose to patients undergoing radiologic examinations. The major benefit of using the effective dose is that this parameter accounts for the absorbed doses and relative radiosensitivities of the irradiated organs in the patient and, therefore, better quantifies the patient risk.[3–5] Unfortunately, the effective dose is difficult to determine because it generally requires a knowledge of the mean absorbed dose to each irradiated organ in the body.[6,7] The energy imparted to the patient, also known as the integral dose, is a measure of the total ionizing energy deposited in the patient during a radiologic examination and may be used to quantify the patient dose in diagnostic radiology.[8–10] In general, energy imparted is easier to calculate or measure than the effective dose.[11] The energy imparted to a patient may be used directly as an approximate indicator of the patient risk[9,12] or used to estimate the corresponding values of the effective dose equivalent.[13]

The energy imparted during a radiologic examination may be obtained from measured depth dose data[11,14,15] and methods derived from this approach.[16,17] Energy imparted generally depends on the x-ray beam quality, as well as the field size and irradiation geometry, which makes depth dose data of limited value in the everyday clinical setting. Monte Carlo techniques may also be used to obtain values of energy imparted, but these methods are computer intensive, time consuming, and relatively cumbersome to use.[18,19] The most practical approach developed to date to obtain values of energy imparted is the use of transmission ionization chambers, which can generate energy imparted data from an exposure-area, or air collision kerma-area product.[20] Measurements of exposure-area product have been reported to result in an accuracy of energy imparted between 10% and 20%.[20,21] However, exposure-area product meters do not take into account the patient thickness, and the incident beam may not totally irradiate the patient. Although it may be possible to overcome both of these limitations, an accurate and practical method for estimating energy imparted to patients that does not rely on special instrumentation would clearly be advantageous.

In this study, we describe a method to obtain an estimate of the energy imparted to patients undergoing radiologic examinations, which may be used with the dosimetry equipment available in most radiology departments. The method is

 0094-2405/97/24(4)/571/9/$10.00

based on Monte Carlo calculations of energy imparted from monoenergetic photons[19] and makes use of published diagnostic energy x-ray spectra.[22] The patient is modeled as a homogenous slab of water with a specified thickness. The water equivalence of a given patient may be obtained by direct measurement of the patient or by estimating the thickness of water that results in the same x-ray technique factors when the imaging equipment is in automatic exposure control (AEC) mode. Experimental measurements needed for this computation include the entrance skin exposure, the x-ray beam qualities (kV and HVL), as well as the exposed area and thickness of the patient, all of which may be readily measured or otherwise estimated. The results of our method for obtaining the energy imparted to patients undergoing representative diagnostic examinations were compared with the corresponding values of energy imparted obtained using Monte Carlo dosimetry techniques with an anthropomorphic phantom.

II. METHOD

A. X-ray spectra

A semi-empirical model developed by Tucker *et al.*[22] was used to compute x-ray spectra generated by energetic electrons hitting an alloy target of tungsten mixed with 10% rhenium atoms. X-ray spectra were generated at tube voltages ranging from 50 to 140 kV using x-ray tube filtration ranging from 1 to 6 mm aluminum (Al). The generated x-ray spectra consisted of discrete energy bins, $\Phi(E)$, each giving the number of x-ray photons per unit area at a given distance from the source in the energy interval between $E-1$ and E keV.

The waveform ripple factor, f, of an x-ray generator may be expressed as

$$f=\frac{V_p-V_l}{V_p}, \tag{1}$$

where V_p and V_l are the maximum (peak) and minimum x-ray tube voltages. The effect of a varying x-ray tube voltage on the output x-ray spectrum was accounted for by using the idealized waveform ripple shown in Fig. 1.[23] The value of the minimum V_l was rounded to the nearest integer, V_l', and the voltage range between V_l' to V_p was subdivided into equal increments of 1 kV. X-ray spectra were generated at each voltage increment and were summed to yield the x-ray spectrum for a given waveform. The time intervals, $\delta(t)_i$, during which the tube voltage increases from V_i to V_{i+1} (Fig. 1) was obtained using the expression

$$\delta(t)_i=\sin^{-1}\left(\frac{V_{i+1}}{V_p}\right)-\sin^{-1}\left(\frac{V_i}{V_p}\right). \tag{2}$$

The total time, $\Delta(t)$, for the voltage to increase from V_l' to V_p was obtained using the expression

$$\Delta(t)=\sin^{-1}\left(\frac{V_p}{V_p}\right)-\sin^{-1}\left(\frac{V_l'}{V_p}\right). \tag{3}$$

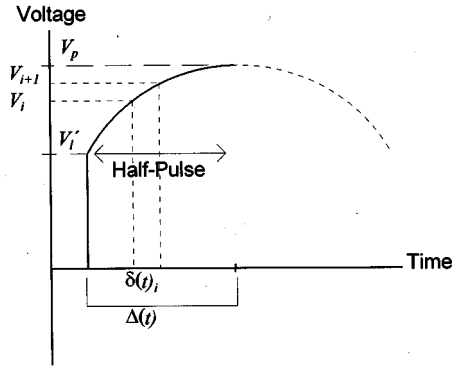

FIG. 1. Schematic diagram of a half-pulse section of the kilovolt waveform ripple. The tube voltage is taken to fluctuate between V_l' and V_p; $\delta(t)_i$ is the time interval of the ith ripple section; $\Delta(t)$ is the total time it takes the ripple waveform to reach from V_l' to V_p.

The x-ray spectrum for a given waveform ripple was obtained using the expression

$$\Phi(E)=\sum_{i=V_l'}^{V_p}\frac{\delta(t)_i}{\Delta(t)}\Phi_i(E), \tag{4}$$

where $\Phi_i(E)$ is the x-ray spectrum generated at a voltage V_i. Equation (4) was used to generate x-ray spectra for x-ray tube voltage ripple factors ranging from 0% (i.e., constant potential) to 100% (i.e., single phase).

X-rays generated at a depth inside the target undergo attenuation by the target material and for a given voltage, changes in the anode angle will alter the beam quality (i.e., degree of beam hardening) of the resultant x-ray spectrum. Tucker *et al.*[22] developed an expression to account for self-attenuation in the target as a function of the tube anode angle that was employed in this study to obtain x-ray spectra for anode angles ranging from 6° to 20°.

B. Entrance exposure and HVL

The exposure in air for an x-ray spectrum with discrete energy bins, $\Phi(E)$, generated at a tube voltage V was obtained using the expression

$$X=\frac{e}{W}\sum_{E=1}^{V}\frac{\mu_{ab}(E)}{\rho_{\text{air}}}E\Phi(E)\quad\frac{\text{C}}{\text{kg}}, \tag{5}$$

where e is the unit charge, W is the ionization energy of air, and $\mu_{ab}(E)/\rho_{\text{air}}$ is the mass energy absorption coefficient of air. The ionization energy of air was taken to be 33.97 eV per ion pair.[22] The exposure X in C/kg was converted to roentgens using the relationship $1.0\,\text{R}=2.58\times10^{-4}\,\text{C/kg}$. The HVL of an x-ray spectrum generated at a tube voltage V was obtained using an iterative method by varying the aluminum filtration thickness until the resultant x-ray beam exposure was reduced to 50% of the original value. The iterative process of computing the HVL resulted in an uncertainty of the HVL of no more than 0.01 mm.[23]

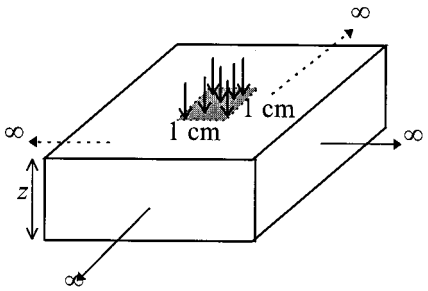

FIG. 2. X-ray irradiation geometry of a semi-infinite water phantom with a thickness of z cm.

C. Energy imparted: Water phantom

Figure 2 shows the irradiation geometry assumed for the computation of energy imparted. For a semi-infinite water phantom of thickness z cm, irradiated normally by an x-ray spectrum generated at an x-ray tube voltage V, the energy imparted due to a uniform x-ray beam with 1 cm^2 cross-sectional area may be obtained from the expression

$$\epsilon(z)=\sum_{E=1}^{V}\epsilon(E,z)\Phi(E)\quad \frac{\mathrm{J}}{\mathrm{cm}^2}, \tag{6}$$

where $\epsilon(E,z)$ is the average energy in joules imparted to the water phantom with thickness z cm by a normally incident monoenergetic photon of energy E. Polynomial expressions from Boone[19,24] were used to compute $\epsilon(E,z)$ over the energy range of 10–145 keV at increments of 1 keV.

For any diagnostic x-ray spectrum, the energy imparted per unit exposure-area product, $\omega(z)$, is the energy imparted to the phantom of thickness z, for an x-ray beam with a cross-sectional area of 1 cm^2, normalized to unit exposure (free-in-air) at the phantom surface with no backscatter. Values of energy imparted per unit area-exposure product, $\omega(z)$, were obtained by dividing Eq. (6) by Eq. (5), yielding

$$\omega(z)=\frac{W}{e}\frac{\Sigma_{E=1}^{V}\epsilon(E,z)\Phi(E)}{\Sigma_{E=1}^{V}(\mu_{ab}/\rho_{\mathrm{air}})_E E\Phi(E)}\quad \frac{\mathrm{J}}{\mathrm{R\ cm}^2}. \tag{7}$$

Values of energy imparted per unit area-exposure product were computed from x-ray spectra generated at constant voltages, ranging from 50 to 140 kV using a tube anode angle of 12°. Added tube filtration ranged from 1 to 6 mm aluminum in increments of 0.5 mm. Computations of $\omega(z)$ were made for water phantom thicknesses ranging from 5 to 30 cm in increments of 5 cm.

D. Energy imparted: Anthropomorphic phantom

The results of energy imparted computations for representative radiologic examinations using the method described in this study were compared with corresponding energy imparted values determined from dosimetry data based on Monte Carlo calculations performed on an anthropomorphic phantom.[7] These Monte Carlo data provide values of the mean doses to three body regions [i.e., head (5.8 kg), trunk including arms (43.0 kg), and legs (22.1 kg)],[25] which permit the energy imparted to each body region to be determined from the product of the mean dose and mass of the specified body region. The energy imparted, ϵ, to the anthropomorphic phantom was computed using

$$\epsilon=D_h m_h+D_t m_t+D_l m_l, \tag{8}$$

where D_h, D_t, and D_l denote the average absorbed doses in the head, trunk, and leg regions, respectively, and m_h, m_t, and m_l are the corresponding masses of these body regions. Anterio–posterior and lateral view examinations covering the head, chest, stomach, and rectum were investigated. The published dosimetry data of Hart *et al.*[7] are normalized to unit air dose-area product (free-in-air) and the relationship that an exposure of 87.7 R results in an air dose of 1.0 Gy was used to convert air absorbed dose values to exposure. Typical entrance skin exposures (free-in-air) were assumed for each examination (listed in Fig. 8) with the x-ray beam cross-sectional area at the patient midplane obtained from

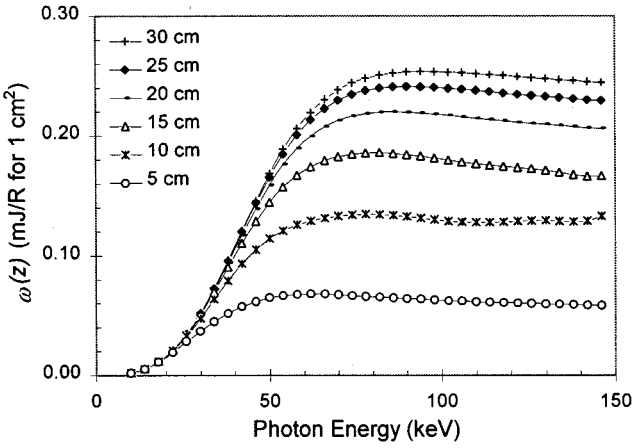

FIG. 3. Values of $\omega(z)$ (mJ R^{-1} cm^{-2}) as a function of photon energy of monoenergetic photons for water phantoms with thicknesses from 5 to 30 cm.

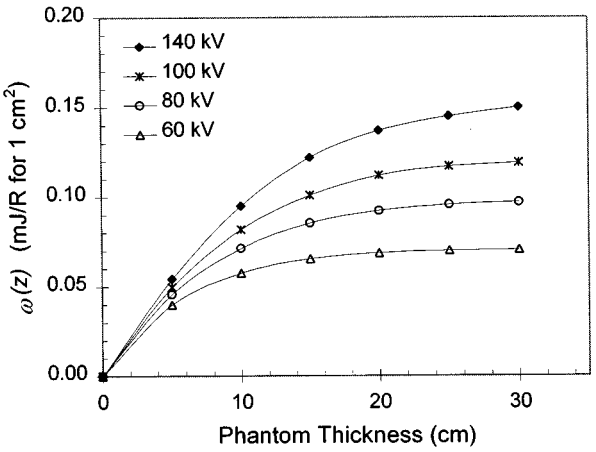

FIG. 4. Values of $\omega(z)$, computed using Eq. (7), for a constant x-ray tube potential 3 mm Al filtration and an anode angle of 12° plotted as a function of water phantom thickness.

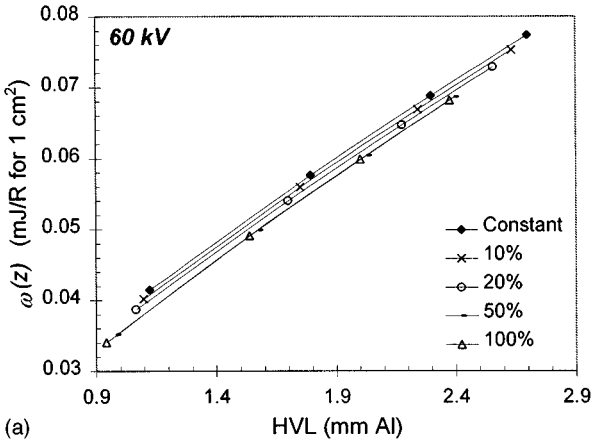

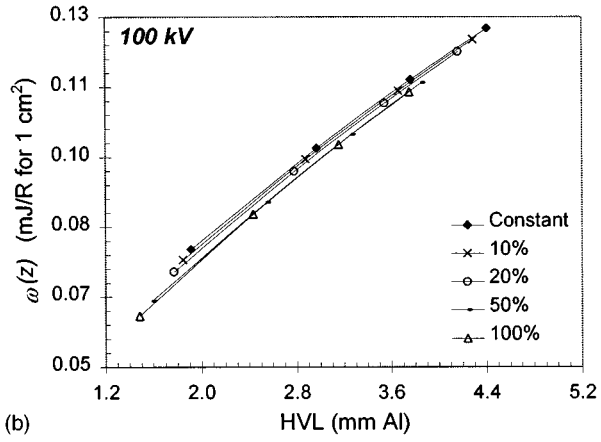

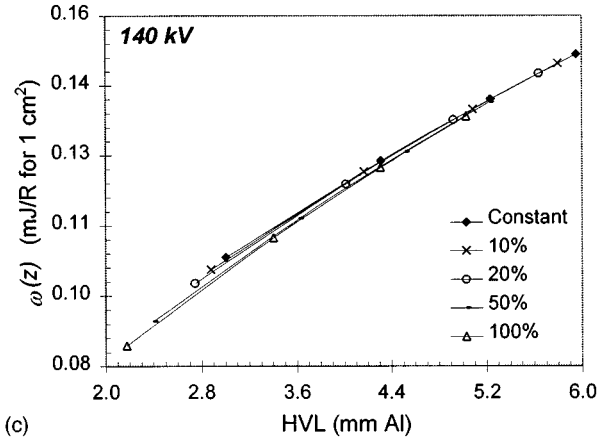

FIG. 5. Values of $\omega(z)$ as a function of HVL for a water phantom thickness of 20 cm.

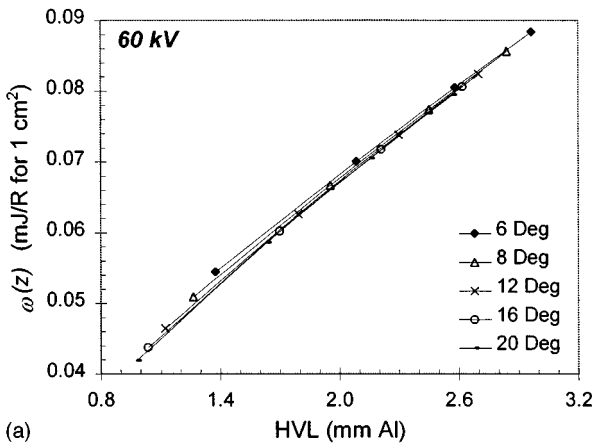

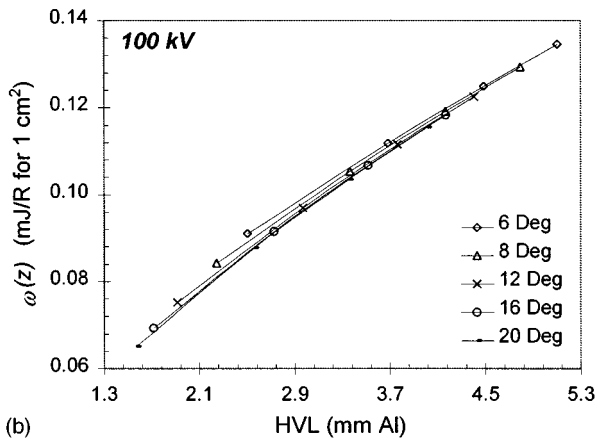

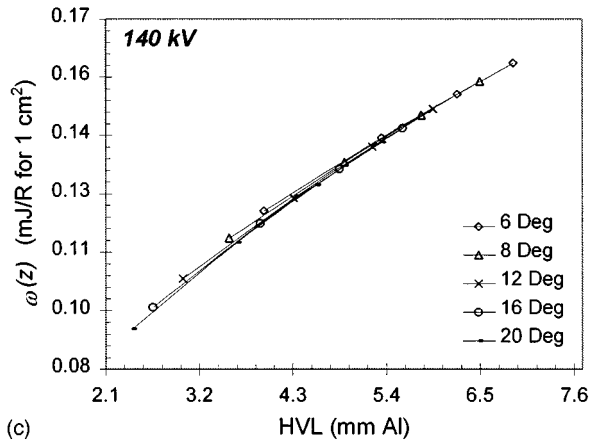

FIG. 6. Values of $\omega(z)$ as function of the HVL for a water phantom of 20 cm.

the published data of Hart *et al.*[7] Inverse square law corrections were applied, using the specified SID/SSD data, to obtain the x-ray beam area at the patient entrance and appropriate corrections were incorporated for the fraction of the x-ray beam that intercepted the patient.[26]

III. RESULTS

Figure 3 shows the computed values of energy imparted per unit exposure-area product, obtained using Eq. (7), for monoenergetic photons as a function of photon energy. Values of $\omega(z)$ always increased with increasing water phantom thickness. For a given water phantom thickness, the $\omega(z)$ parameter initially increased before reaching an approximately constant plateau value. Figure 4 shows $\omega(z)$ computed using Eq. (7) as a function of phantom thickness for x-ray spectra generated at constant x-ray tube voltages ranging from 60 to 140 kV and an anode angle of 12°. The

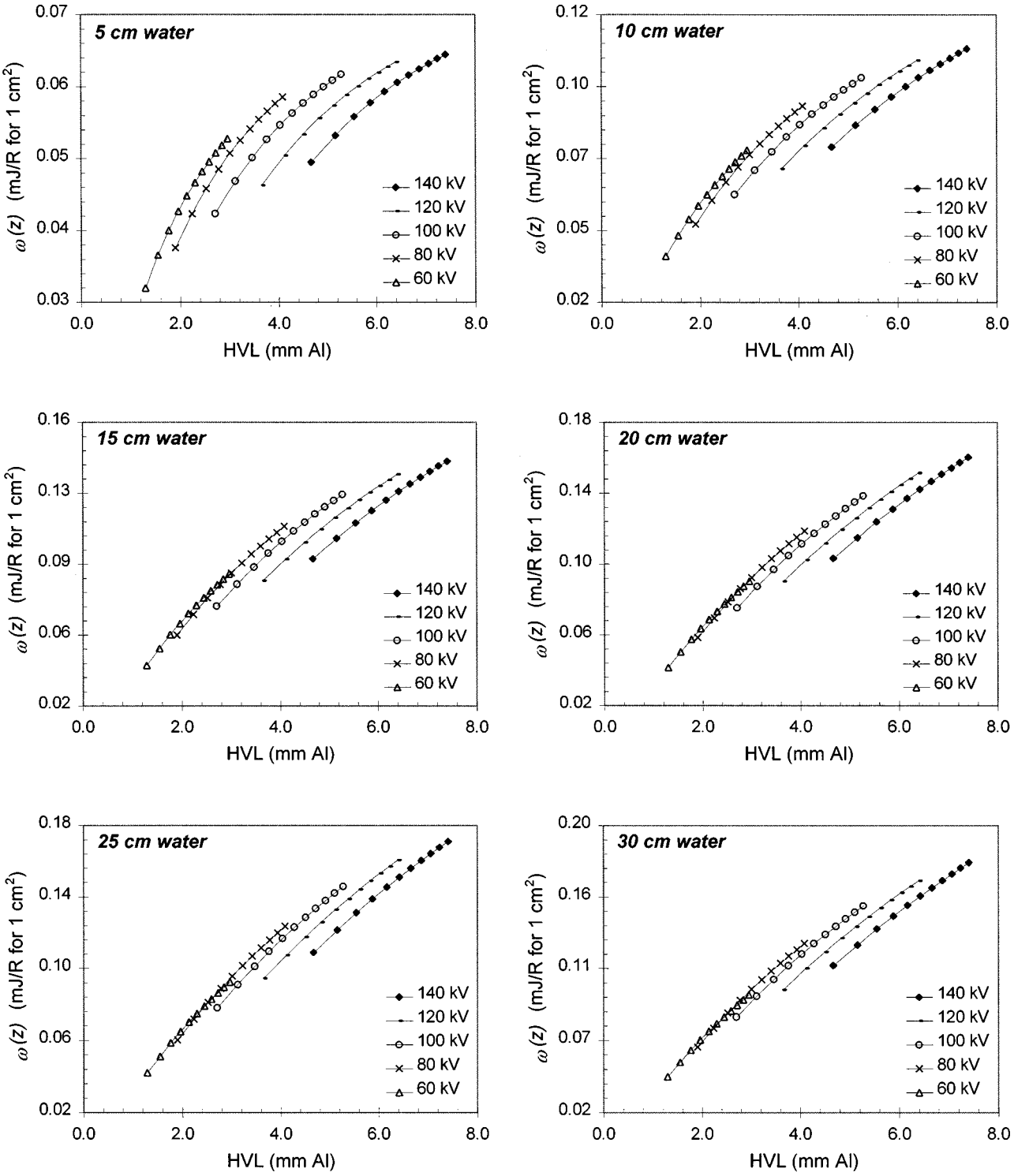

FIG. 7. Values of $\omega(z)$ as a function of HVL for water phantoms with a thickness of 5–30 cm.

increase of $\omega(z)$ with phantom thickness is largest at the smallest phantom thicknesses. For a phantom thickness of 20 cm at 80 kV, variations of phantom thickness of $\pm$ 0.5 cm would change $\omega(z)$ by only $\pm$ 0.5%. At the same kV, however, a variation of $\pm$ 0.5 cm for a nominal phantom thickness of 5 cm would change $\omega(z)$ by $\pm$ 7.0%.

Figure 5 shows values of $\omega(z)$ plotted as a function of the HVL for voltage waveform ripples between 0% and 100%. For a given x-ray tube voltage, $\omega(z)$ increased linearly with the HVL. At a given tube voltage and HVL, the waveform ripple had a minor impact on the value of $\omega(z)$. At 60 kV, going from a constant potential to a single phase generator reduced the value of $\omega(z)$ by less than 4%, and at 140 kV, this change was less than 1%. For modern x-ray generators

with ripple factors, ranging from 0% to 20%, neglecting any waveform ripple when computing a value of $\omega(z)$ would result in errors of between 0% and 2% for any given kV and HVL. Figure 6 shows values of $\omega(z)$ plotted as a function of the HVL for anode angles between 6° and 20°. For a given x-ray tube voltage, $\omega(z)$ increased linearly with the HVL. At a given tube voltage and HVL, the anode angle had a minor impact on the value of $\omega(z)$, and changing the anode angle from 6° to 20° affected the value of $\omega(z)$ by less than 2%.

Figure 7 shows the values of $\omega(z)$ computed using Eq. (7) for constant x-ray tube voltages and an anode angle of 12° plotted as a function of the HVL. At a given tube voltage and phantom thickness, $\omega(z)$ increased linearly with the HVL. For each tube voltage and phantom thickness, values of $\omega(z)$ were fitted to the equation

$$\omega(z) = \alpha \times \mathrm{HVL} + \beta \quad \mathrm{J\,R^{-1}\,cm^{-2}} \tag{9}$$

where α and β are parameters of the fit. Table I lists the resultant values of α and β parameters for each listed kV and phantom thickness. All the correlation coefficients, r^2, obtained for these linear fits ranged between 0.984% and 1.00. All values of $\omega(z)$ computed using the α and β parameters listed in Table I agree to within 1.9% when compared to the exact values obtained using Eq. (7).

Figure 8 shows values of energy imparted as a function of tube voltage for four body regions and two projections with an x-ray tube filtration of 3 mm Al, where the data points have been fitted to a second-order polynomial. In each figure, the water equivalent phantom thickness assumed in our computation is provided with the error bars indicating the variations in energy imparted obtained by changing the water phantom thickness by $\pm$ 2 cm. For water phantom thickness values not listed in Table I, the appropriate $\omega(z)$ values were obtained from a polynomial fit of $\omega(z)$ plotted as a function of phantom thickness. For the same entrance exposure, values of energy imparted increased with increasing tube voltage and filtration. At 60 kV, the average difference between the two methods of determining energy imparted was 8% with a maximum difference of 20% for the LAT Stomach examination. At 80 kV, the average difference between the two methods was 10% with the maximum being 25% for the LAT Stomach examination. At 120 kV, the two methods produced results with an average difference of 12%, with the LAT Stomach examination resulting in a maximum difference of 29%.

IV. DISCUSSION

Figure 3 shows that for a given phantom thickness, the value of the energy imparted per unit exposure-area product, $\omega(z)$, is strongly dependent on photon energy at the lower photon energies. As the photon energy increases, however, the value of $\omega(z)$ generally reaches a plateau value and becomes relatively independent of photon energy. This behavior indicates that for heavily filtered x-ray beams at high kV's, the energy imparted to the phantom normalized to the entrance skin exposure will be relatively independent of the x-ray spectrum. If the x-ray spectrum contains lower-energy photons, it is the factors that harden an x-ray beam (e.g., small tube anode angles) that will cause $\omega(z)$ to increase, while factors that soften the x-ray beam (e.g., large ripple factors) will reduce $\omega(z)$.

Figure 4 shows the energy imparted per unit exposure-area product, $\omega(z)$, as a function of phantom thickness for a range of x-ray tube voltages. The largest increase of $\omega(z)$ with phantom thickness is expected at small thicknesses, given that the mean-free path of monoenergetic photons in water ranges from 4.4 cm at 50 keV to 6.6 cm at 140 keV. Once the phantom thickness reaches about three or four mean-free paths, most of the x-ray photons will have been absorbed and any further increase of the phantom thickness will have little affect on $\omega(z)$. Figure 4 shows that at 80 kV, the thickness of the water phantom used to simulate a patient for the purposes of estimating energy imparted generally will not be a critical parameter for applications with phantom thicknesses greater than 10 cm. For phantom thicknesses less than 10 cm, however, the selection of phantom thickness will be more important.

The energy imparted, ϵ, to a patient undergoing a radiologic examination, can be estimated by modeling the patient as a slab of water. A knowledge (or measurement) of the x-ray beam kV and HVL, together with an estimate of the

TABLE I. Values of α and β parameters for different tube voltages and phantom thicknesses. At a given kV, values of $\omega(z)$ to a water phantom with thickness z cm are given by $\omega(z) = \alpha \times \mathrm{HVL} + \beta$, where the HVL is expressed in mm Al and $\omega(z)$ is in J R^{-1} cm^{-2}.

	Phantom thickness											
	5 cm		10 cm		15 cm		20 cm		25 cm		30 cm	
kV	α	β	α	β	α	β	α	β	α	β	α	β
50	1.08E−05	1.44E−05	1.80E−05	1.36E−05	2.11E−05	1.26E−05	2.23E−05	1.21E−05	2.28E−05	1.19E−05	2.29E−05	1.18E−05
60	9.20E−06	1.80E−05	1.65E−05	1.89E−05	2.03E−05	1.84E−05	2.19E−05	1.79E−05	2.27E−05	1.76E−05	2.29E−05	1.75E−05
70	8.04E−06	2.10E−05	1.52E−05	2.38E−05	1.94E−05	2.39E−05	2.14E−05	2.36E−05	2.23E−05	2.34E−05	2.27E−05	2.32E−05
80	6.98E−06	2.39E−05	1.38E−05	2.88E−05	1.81E−05	3.01E−05	2.04E−05	3.02E−05	2.14E−05	3.02E−05	2.19E−05	3.01E−05
90	6.13E−06	2.63E−05	1.26E−05	3.33E−05	1.69E−05	3.57E−05	1.93E−05	3.64E−05	2.05E−05	3.66E−05	2.10E−05	3.67E−05
100	5.42E−06	3.85E−05	1.15E−05	3.75E−05	1.57E−05	4.12E−05	1.80E−05	4.26E−05	1.93E−05	4.31E−05	1.99E−05	4.33E−05
110	4.82E−06	3.04E−05	1.05E−05	4.14E−05	1.45E−05	4.64E−05	1.68E−05	4.85E−05	1.81E−05	4.94E−05	1.87E−05	4.98E−05
120	4.35E−06	3.21E−05	9.68E−06	4.47E−05	1.35E−05	5.08E−05	1.58E−05	5.36E−05	1.71E−05	5.48E−05	1.77E−05	5.53E−05
130	3.95E−06	3.35E−05	8.96E−06	4.78E−05	1.26E−05	5.50E−05	1.49E−05	5.83E−05	1.61E−05	5.99E−05	1.68E−05	6.06E−05
140	3.61E−06	3.48E−05	8.36E−06	5.05E−05	1.18E−05	5.86E−05	1.41E−05	6.25E−05	1.53E−05	6.44E−05	1.60E−05	6.53E−05

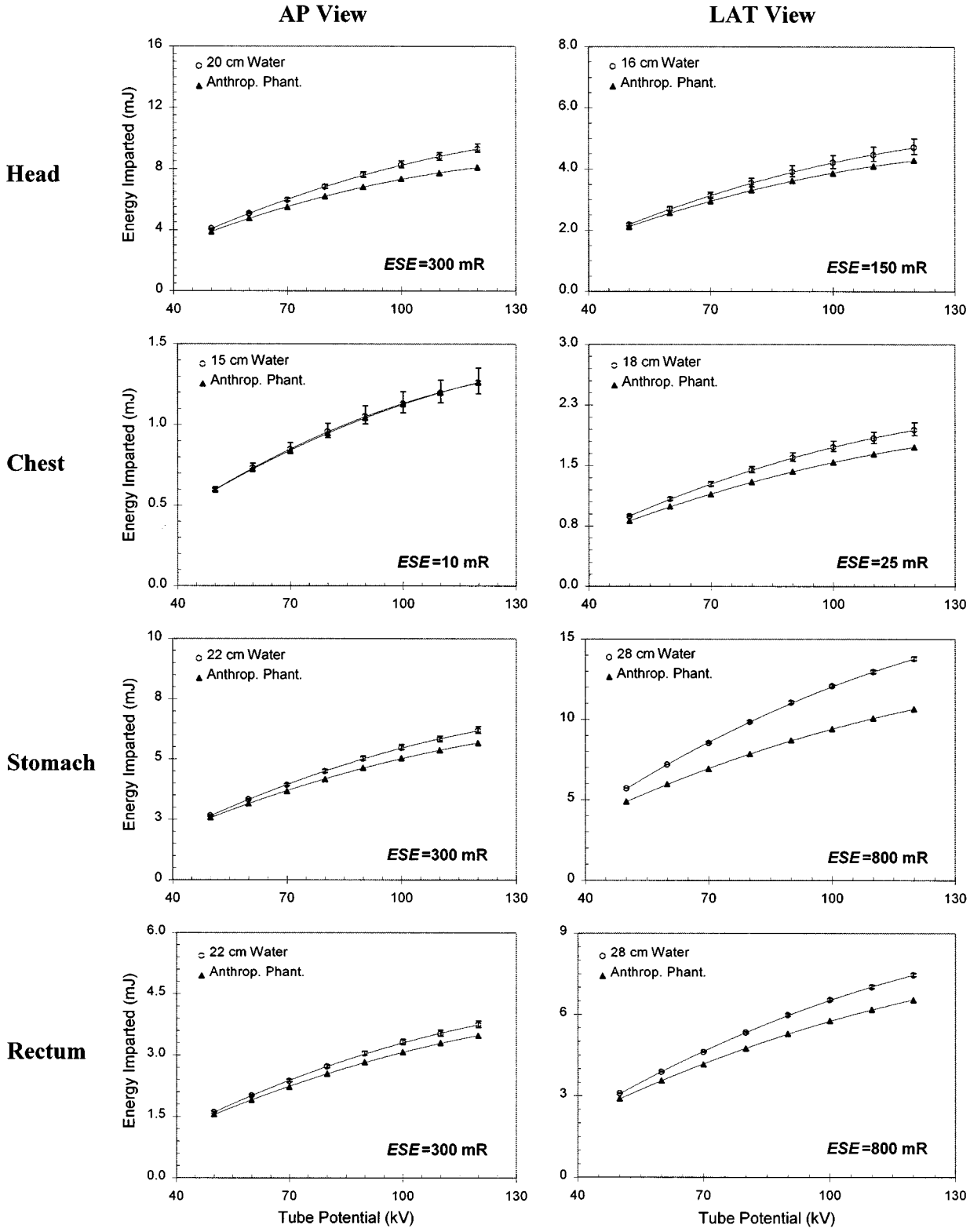

FIG. 8. Energy imparted as a function of tube voltage for representative x-ray examinations. The entrance skin exposures, ESE, values (free in air) used for each calculation are listed in each figure.

water equivalent thickness, z, of the patient will permit the appropriate value of $\omega(z)$ to be determined. The product of the free-in-air exposure at the patient entrance surface and the x-ray beam area at this location yields the exposure-area product, EAP. The energy imparted to the patient may then be computed using the expression $\epsilon = \omega(z) \times \text{EAP}$. An exposure area meter mounted at the collimator of the x-ray tube may also be used to obtain a direct estimate of the EAP.[27–30]

TABLE II. Entrance skin exposure, energy imparted, and effective dose equivalent for representative radiologic examinations of the head, chest, abdomen, and pelvis.

Exam	Projection	z (cm)	kVp/HVL (kV/mm Al)	Beam area (cm^2)	ESE[a] (mR[b])	ϵ (mJ)	H_E (μSv)
Head	PA	20	80/3.0	250	300	6.8	67
	LAT	16	75/2.8	270	150	3.3	35
Chest	PA	15	120/5.8	1100	10	1.4	19
	LAT	18	120/5.8	640	25	2.3	46
	AP portable	15	80/3.0	960	20	1.9	47
Abdomen	AP	23	75/2.8	900	300	23	480
Lumbar spine	AP	23	75/2.8	700	300	18	450
	LAT	28	80/3.0	240	800	18	210
Pelvis/colon	AP	23	75/2.8	840	300	22	590
Fluoroscopy (1 min)	PA	23	80/3.0	200	3000	56	600

[a]Free in air.
[b]1.0 R=2.58E−4 C/kg.

Any EAP measurements, however, will need to be corrected to take into account the fraction of the x-ray beam area that actually intercepts the patient.

Our method to estimate energy imparted to patients undergoing diagnostic x-ray examinations has several sources of error. Minor errors in computing energy imparted to patients arise from the use of diverging x-ray beams in clinical radiography and the presence of nonuniformities in x-ray beam intensity due to the heel effect. The former is likely to be of negligible importance whereas the latter could easily be accounted for by experimentally obtaining an average entrance skin exposure over the beam area. This latter method is explicitly done when an exposure-area meter is used to quantify the amount of radiation incident on the patient.

Major errors in determining energy imparted to patients result when estimating the equivalent water phantom thickness, z, and due to the implicit differences between a (finite) heterogenous patient and a semi-infinite homogeneous water phantom (Fig. 2). The data presented in Fig. 4 and Fig. 8 indicate that for many clinical applications, the precise value of the water phantom thickness has a small effect on the resultant value of energy imparted. The data presented in Fig. 8 show very good agreement at the lowest kV values, whereas at higher kV's, the water phantom model generally overestimated the energy imparted values. Given that (lateral) scatter becomes increasingly important at higher kV values, these results suggest that the major source of error may be the use of a water phantom model with infinite lateral extent.

Table II shows a summary of the energy imparted values to patients undergoing a number of radiologic examinations. These values of energy imparted are only approximate indicators of patient risk since they do not take into account the radiosensitivities of the irradiated organs or the age demographics of the irradiated patients.[31] Nevertheless, studies have shown that energy imparted can correlate reasonably well with patient risk for examinations ranging from chest x rays to barium enemas.[9] For uniform whole body exposure in an adult reference man (70 kg), an absorbed energy of 1 J would correspond to an effective dose of 14 mSv. For nonuniform irradiation normally encountered in diagnostic radiology, energy imparted data may be converted into effective dose equivalents by using body region specific H_E/ϵ conversion factors,[13] which were used to generate the data in the last column of Table II. Energy imparted to a patient examination range from a few mJ for simple chest examinations to several hundreds of mJ for fluoroscopic examinations lasting ten minutes. The corresponding values of effective dose equivalent range from tens of μSv to tens of mSv.

Energy imparted to patients undergoing diagnostic examinations may be used to study the relationship between the image quality and the patient dose,[32–35] particularly with the advent of digital radiographic imaging equipment such as photostimulable phosphors and photoconductors.[36] Digital detectors normally permit the radiation exposure to be freely selected by the operator, as opposed to fixed exposures required to generate satisfactory radiographs screen-film combinations. As a result, a simple and convenient method for estimating patient doses permits a systematic investigation of how patient dose and image quality change as radiographic technique factors change. The patient dosimetry method developed in this study is well suited for this purpose since it requires a minimum of effort and no special measurement equipment beyond that normally found in diagnostic radiology departments and has an accuracy that is likely to be satisfactory for most patient dosimetric applications.

ACKNOWLEDGMENTS

We are grateful to Dr. Douglas M. Tucker for assisting with the computation of the x-ray spectra, Dr. John Boone for providing us with updated data on energy imparted for monoenergetic photons, and Linda Waters-Funk for preparing the final manuscript.

[a)]Corresponding author: Phone: (352) 395-0293; Fax: (352) 395-0279; Electronic mail: hudaw@xray.ufl.edu

[1]International Committee on Radiation Protection, *ICRP Publication 26: Annals of the ICRP, 1977 Recommendation of the International Commission on Radiological Protection* (Pergamon, New York, 1977).

[2]International Committee on Radiation Protection, *ICRP Publication 60: Annals of the ICRP, 1990 Recommendation of the International Commission on Radiological Protection* (Pergamon, New York, 1991).
[3]United Nations Scientific Committee on the Effects of Atomic Radiation, *1988 Report: Sources, Effects and Risk of Ionizing Radiation* (United Nations, New York, 1988).
[4]National Council on Radiation Protection, *Report 100: Exposure of the US Population from Diagnostic Medical Radiation* (National Council on Radiation Protection and Measurements, Bethesda, MD, 1989).
[5]International Committee on Radiation Protection, *ICRP Publication 53: Annals of the ICRP, Radiation Dose to Patients from Radiopharmaceuticals* (Pergamon, New York, 1987).
[6]W. Huda, G. Sandison, R. Palser, and D. Savoie, ''Radiation doses and detriment from chest x-ray examinations,'' Phys. Med. Biol. **34**, 1477–1492 (1989).
[7]D. Hart, D. Jones, and B. Wall, *NRPB SR262: Normalized Organ Doses for Medical X-ray Examinations Calculated Using Monte Carlo Techniques* (National Radiological Protection Board, Chilton, Oxon, UK, 1994).
[8]B. Wall, E. Fisher, R. Paynter, A. Hudson, and P. Bird, ''Doses to patients from pantomographic and conventional dental radiography,'' Br. J. Radiol. **52**, 727–734 (1979).
[9]B. Wall, R. Harrison, and F. Spiers, *ISPM Report #53: Patient Dosimetry Techniques in Diagnostic Radiology* (The Institute of Physical Science in Medicine, York, UK, 1988).
[10]W. Huda, J. McLellan, and Y. McLellan, ''How will the new definitions of 'effective dose' modify estimates of dose in diagnostic radiology?,'' J. Radiat. Protect. **11**, 241–247 (1991).
[11]C. Carlsson, ''Determination of integral absorbed dose from exposure measurements,'' Acta Radiol. **1**, 433–458 (1963).
[12]J. Cameron, ''Dose equivalent out—Imparted energy in,'' HPS Newsletter, 1992, pp. 7–8.
[13]W. Huda and K. Bissessur, ''Effective dose equivalents, H_E, in diagnostic radiology,'' Med. Phys. **17**, 998–1003 (1990).
[14]C. Carlsson, ''Integral absorbed doses in roentgen diagnostic procedures. I. The dosimeter,'' Acta Radiol. Ther. Phys. Biol. **3**, 310–326 (1965).
[15]R. Harrison, ''A re-evaluation of the 'saturated scatter' method for estimating the energy imparted to patients during diagnostic radiology examinations,'' Phys. Med. Biol. **28**, 701–707 (1983).
[16]R. Hummel, R. Wesenberg, and G. Amundson, ''A computerized x-ray dose-monitoring system,'' Radiology **156**, 231–234 (1985).
[17]G. Carlsson, C. Carlsson, and J. Persliden, ''Energy imparted to the patients in diagnostic radiology: Calculation of conversion factors for determining the integral dose from measurements of the air collision kerma integrated over beam area,'' Phys. Med. Biol. **29**, 1329–1341 (1984).
[18]J. Persliden and G. Carlsson, ''Energy imparted to water slabs by photons in energy range 5–300 keV: Calculations using Monte Carlo photon transport model,'' Phys. Med. Biol. **29**, 1075–1088 (1984).
[19]J. Boone, ''Parametrized x-ray absorption in diagnostic radiology from Monte Carlo calculations: Implications for x-ray detector design,'' Med. Phys. **19**, 1467–1473 (1992).
[20]P. Shrimpton, B. Wall, D. Jones, and E. Fisher, ''The measurement of energy imparted to patients during diagnostic x-ray examinations using the Diamentor exposure-area product Meter,'' Phys. Med. Biol. **19**, 1199–1208 (1984).
[21]B. Berthelsen and Å Cederblad, ''Radiation doses to patients and personnel involved in embolization of intracerebral arteriovenous malformations,'' Acta Radiol. **32**, 492–497 (1991).
[22]M. Tucker, G. Barnes, and D. Chakraborty, ''Semi-empirical model for generating tungsten target x-ray spectra,'' Med. Phys. **18**, 211–218 (1991).
[23]N. Gkanatsios, *Master Thesis: Computation of Energy Imparted in Diagnostic Radiology* (University of Florida, Gainesville, FL, 1995).
[24]J. Boone (private communication, 1994).
[25]B. Wall (private communication, 1996).
[26]D. Jones and B. Wall, *NRPB R186: Organ Doses from Medical X-ray Examinations Calculated Using Monte Carlo Techniques* (National Radiological Protection Board, Chilton, Oxon, UK, 1985).
[27]K. Faulkner, H. Busch, P. Cooney, J. Malone, N. Marshall, and D. Rawlings, ''An international intercomparison of dose-area product meters,'' Radiat. Protect. Dosim. **43**, 131–134 (1992).
[28]P. Kichen, G. Kemerink, P. Vaessen, and J. Ackermans, ''An automated measurement system for characterization of patient exposure during angiography,'' Radiat. Protect. Dosim. **43**, 165–169 (1992).
[29]L. Wagner, ''Studies on the performance of diagnostic ionization air kerma meters in the United States,'' Radiat. Protect. Dosim. **43**, 127–130 (1992).
[30]R. Harrison, K. Faulkner, M. Davies, C. Chapple, K. Robson, and D. Broadhead, ''Patient dosimetry in diagnostic radiology—Some practical considerations in an NHS region,'' J. Radiol. Protect. **15**, 203–216 (1995).
[31]W. Huda, and J. Bews, ''Population irradiation factors (PIFs) in diagnostic medical dosimetry,'' Health Phys. **59**, 345–347 (1990).
[32]J. Malone, P. Cooney, H. Busch, and K. Faulkner, ''A review of the background to the decision to write-off fluoroscopy equipment in 15 instances—And the impact of patient dose and image quality in practice,'' Radiat. Protect. Dosim. **58**, 249–252 (1994).
[33]M. Sandborg, J. Christoffersson, G. Carlsson, T. Almén, and D. Dance, ''The physical performance of different x-ray contrast agents: Calculations using Monte Carlo model of the imaging chain,'' Phys. Med. Biol. **40**, 1209–1224 (1995).
[34]M. Tapiovaara and M. Sandborg, ''Evaluation of image quality in fluoroscopy by measurements and Monte Carlo calculations,'' Phys. Med. Biol. **40**, 589–607 (1995).
[35]E. Vañó, L. Gonzàlez, E. Guibelalde, J. Fernàndez, A. Calzade, and M. Ruiz, ''Some results from a diagnostic radiology optimization programme in the Madrid area,'' Radiat. Protect. Dosim. **51**, 289–292 (1995).
[36]W. Hendee and J. Trueblood, in *Medical Physics Monograph No. 22: Digital Imaging* (Medical Physics, Madison, WI, 1993).